Journal of Power Sources 268 (2014) 550–556

Contents lists available at ScienceDirect

Journal of Power Sources

journal homepage: www.elsevier.com/locate/jpowsour

Short communication

Influence of M–B (M = Fe, Co, Ni) on aluminum–water reaction

H.X. Meng [a], N. Wang [b, *], Y.M. Dong [a], Z.L. Jia [a], L.J. Gao [a], Y.J. Chai [a, *]

[a] School of Chemistry and Materials Science, Hebei Normal University, Hebei, Shijiazhuang 050024, China
[b] Analysis and Testing Centre, Hebei Normal University, Hebei, Shijiazhuang 050024, China

HIGHLIGHTS

- The chainlike Fe–B catalyst forms a network structure.
- The catalytic activity in the initial Al/H_2O reaction at 45°Cis Fe–B > Ni–B > Co–B.
- Aluminum is rapidly corroded after consecutive additions of Al batches.
- The high concentrations of OH^- in the local domain triggers the corrosion of Al.

ARTICLE INFO

Article history:
Received 16 April 2014
Received in revised form
14 June 2014
Accepted 16 June 2014
Available online 25 June 2014

Keywords:
Hydrogen generation
Hydrolysis reaction
Aluminum corrosion
Catalyst

ABSTRACT

In this work, the aluminum–water reaction induced by Fe–B, Co–B and Ni–B particles was studied. The catalysts were mixtures of the metal boride and metallic particles. The chainlike Fe–B catalyst forms a network structure under the influence of an external magnetic field and has a large specific surface area. Aggregated particles of Co–B and Ni–B catalyst have small specific surface area. Catalytic activity in the initial corrosion of aluminum increases with increasing Fe–B content because of the large specific surface area and the formation of a micro galvanic cell. However, the amount of hydrogen generated slowly decreases with increasing amount of Co–B and Ni–B. The activity of Fe–B, Co–B and Ni–B in the initial Al/H_2O reaction decreases in the order Fe–B > Ni–B > Co–B. The calculated apparent activation energies in the presence of Fe–B, Co–B and Ni catalysts are 38.2, 39 and 29.6 kJ mol^{-1}, respectively. Aluminum is rapidly and completely corroded in a weakly alkaline solution (pH < 10) after consecutive additions of Al batches because of high concentrations of OH^- in the local domain and an increase in the amount of $Al(OH)_3$ precipitate.

1. Introduction

Hydrogen generation though reaction of aluminum in water and aqueous alkaline solution is extensively being studied because of its safety, cheapness and simplicity. This is one of the mild and easily controlled reactions for the sustainable production of pure hydrogen for use-on-demand systems. However, an inert alumina film that is spontaneously formed on Al surface is stable and prevents the Al/H_2O reaction at neutral pH. This oxide film, which has a thickness of 4–10 nm, is composed of a compact layer of Al_2O_3 and a thin layer of boehmite [γ-AlOOH] or bayerite $Al(OH)_3$ [1].

Several methods have been used to break the alumina film to accelerate hydrogen generation. Soler observed that the addition of $NaSnO_2$ or $NaAlO_2$ to a NaOH solution stimulated the corrosion of Al at high pH or formation of an Al/Sn micro galvanic cell [2,3]. Fan and coworkers studied the hydrogen generation by use of an Al metal mixture with Ga, Bi, In, Sn, Li, Mg or Hg prepared by ball milling [4–6]. They proposed that the improvement of the rate of hydrogen generation rate is related to the formation of a micro galvanic cell or to the production of a soluble hydroxide. Deng investigated the effect of the addition of γ-Al_2O_3 on the corrosion of Al and explained by the uniform corrosion model [7,8]. Dreizin reported that a mixture of Al and oxide (Bi_2O_3, MoO_3, CuO or MgO) prepared by ball milling reacted with water to produce hydrogen via pitting corrosion [9].

* Corresponding authors. Tel.: +86 311 80786451.
E-mail addresses: yjchaiwn@gmail.com, hebsjz407@163.com (Y.J. Chai).

http://dx.doi.org/10.1016/j.jpowsour.2014.06.094
0378-7753/

Amorphous Fe–B, Co–B and Ni–B catalysts have been used in powdered form in studies on $NaBH_4$ hydrolysis in a wide range of conditions. These catalysts, which were prepared through in situ reduction, show high catalytic activity in the hydrolysis of $NaBH_4$ because of their amorphous structure and high surface area [10,11]. Their catalytic activity in alkaline solution decreases in the order: Co–B > Ni–B > Fe–B, as the surface of Co is more favorable for the conversion of $BH_3(OH)^-$ to $B(OH)_4^-$ and for the release of the molecular hydrogen [12]. However, no studies on the catalytic activity of Fe–B, Co–B and Ni–B on the Al/H_2O reaction have been reported. In this work, Fe–B, Co–B and Ni–B were prepared through hydrolysis of $NaBH_4$ in deionized water. Their behavior in Al/H_2O reaction at 45 °C were examined. The effect of Fe–B, Co–B and Ni–B on the initial Al/H_2O reaction was found to decrease in the order Fe–B > Ni–B > Co–B.

2. Experimental

2.1. Preparation of catalyst

Raw aluminum powder (99.0% purity, Tianjin Damao Chemistry Reagent Factory, China, Tianjin), 99.0% $NaBH_4$, and 99.0% $CoCl_2 \cdot 6H_2O$, $FeCl_3 \cdot 6H_2O$, $NiCl_2 \cdot 6H_2O$ (Tianjin Bodi Chemical Co., China) were used in this study.

Fe–B, Co–B and Ni–B catalysts were synthesized through the conventional wet chemical reduction method. These catalysts were typically obtained by adding 0.2 g of borohydride solution to a 20 mL solution containing 0.5 g Fe^{3+}, Co^{2+} or Ni^{2+} ions without stirring. A magnetic stirring bar was used to provide an external magnetic field to collect magnetic particles. Fe–B and Co–B particles, which are strongly ferromagnetic, are attracted to the magnetic stirring bar. Ni–B particles, on the other hand, were separated by filtration because of their weak magnetic property. To remove remaining Na^+ and Cl^- ions, Fe–B, Co–B and Ni–B particles were washed with water and ethanol. Then, it was dried at room temperature.

2.2. Measurement of the amount of generated hydrogen

Fresh catalyst and 0.2 g Al were mixed manually for <5 min. The resulting mixture was transferred to 30 mL dionized water and sealed in a 50 mL flask with stirring. Initial reaction of the mixture was allowed to proceed for 400 min, and then consecutive batches of pristine Al were added to the same flask individually in succession. The byproduct $Al(OH)_3$ was accumulated in this reaction. The flask was heated in a water bath to maintain constant temperature during the entire reaction. The hydrogen produced by the reaction was collected in an inverted burette completely filled with tap water. The volume of hydrogen produced within 400 min was recorded at 10 min intervals from the water-level change in the inverted burette.

2.3. Characterization

The structure of the product was determined on a Bruker D8 Advance X–ray diffractometer (XRD) with Cu Kα radiation at a voltage and current of 40 kV and 40 mA. Surface electronic states and valence state were studied by X-ray photoelectron spectroscopy (XPS, Kratos Axis Ultra DLD multi-technique). The morphology of the products was investigated by means of an S-4800 field–emission scanning electron microscope (FE-SEM). In order to examine the specific area of the byproducts, Brunauer–Emmet–Teller (BET) surface area measurement was performed at −196 °C on NOVA 4000, Quantachrome Corporation.

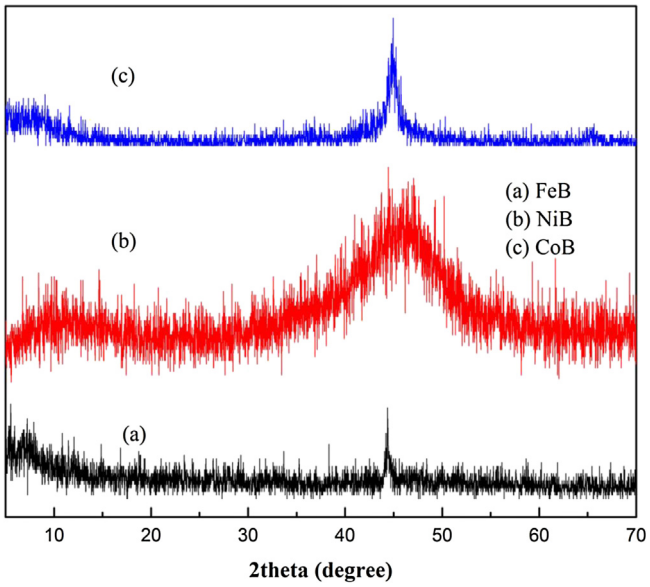

Fig. 1. Typical XRD profiles of Fe–B, Co–B and Ni–B.

3. Results and discussion

3.1. Catalyst characterization

Fig. 1 shows the typical XRD profiles of the fresh Fe–B, Co–B and Ni–B. Typically, they were amorphous. However, the appearance of a peak at 2θ of 45° in the patterns of the Fe–B, Co–B and Ni–B suggests the presence of small amounts of metal Fe, Co and Ni. That is, the catalysts consisted of a mixture of M–B particles (M = Fe, Co, Ni) and reduced metal. The XPS results show that Fe, Co and Ni in the Fe–B, Co–B and Ni–B were in their oxidized state, as evidenced by their binding energies of 711 eV, 782 eV and 853 eV (Fig. 2). No metallic Fe, Co and Ni were detected because of long time storage in the air. This result suggests that the metallic Fe, Co and Ni are not stable in air and are easily oxidized.

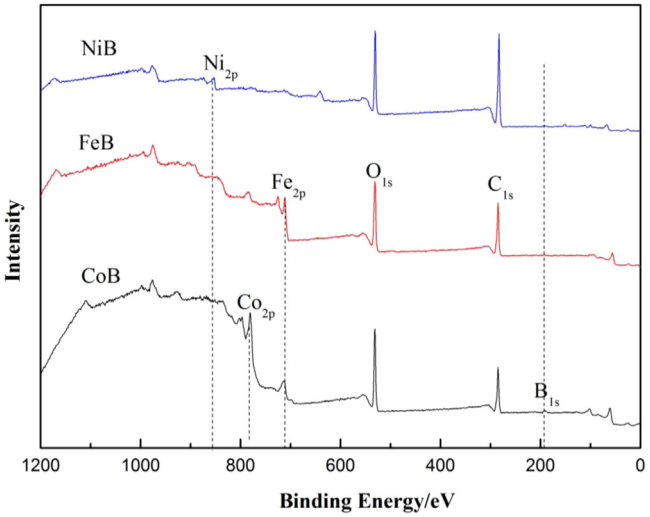

Fig. 2. X-ray photoelectron spectra for Fe–B, Co–B and Ni–B.

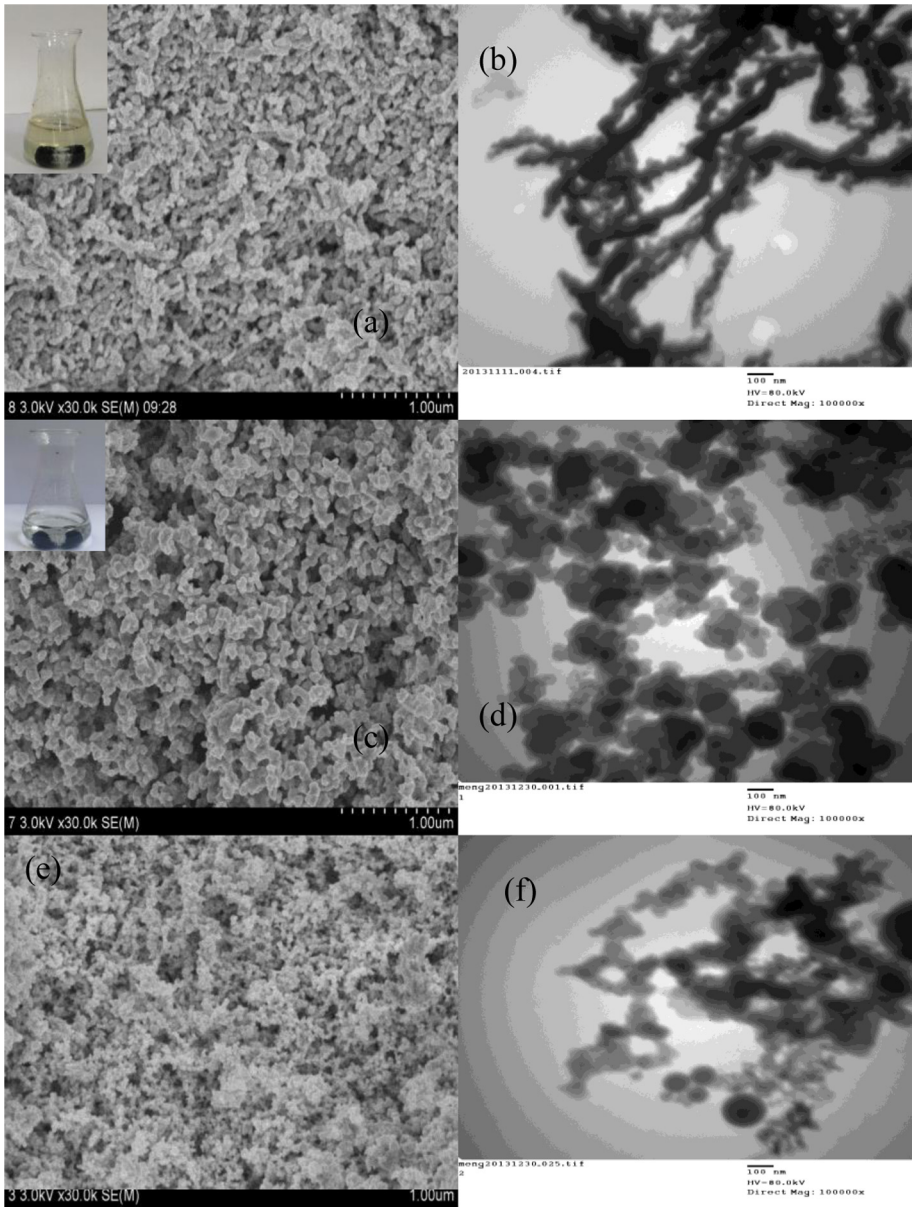

Fig. 3. SEM and TEM images of Fe–B (a,b), Co–B (c,d) and Ni–B (e,f).

Fine Fe–B and Co–B particles were attracted to the magnetic bar (inset of Fig. 3) because of their ferromagnetic property. Fe–B particles aggregated to form a chainlike structure under the external magnetic field (Fig. 3a and b). The chainlike structures linked to form a network structure with a larger specific surface area of (169.7 $m^2\ g^{-1}$, Fig. 4). However, spherical Co–B particles with sizes of <100 nm aggregated. The particles size of Ni–B was smaller than that of the Co–B. The specific surface areas of the Co–B and Ni–B catalysts were 23.6 $m^2\ g^{-1}$ and 21.0 $m^2\ g^{-1}$, respectively, which were much smaller than that of the Fe–B.

3.2. Hydrogen generation induced by Fe–B, Co–B and Ni–B

Fig. 5 shows the amount of hydrogen generated at 45 °C by the Al/H_2O reaction in the presence of Fe–B, Co–B and Ni–B. Almost no hydrogen was generated in the reaction of pristine aluminum with water or the catalysts with water. However, the Al/H_2O reaction was hastened when the amount of Fe–B was increased from 0.01 g to 0.07 g. With this catalyst, the induction time was shortened from ~30 min ($x_{Fe-B} = 0.01$ g) to ~1 min ($x_{Fe-B} = 0.07$ g). The amount of hydrogen generated within 400 min increased from 920 mL g^{-1} to 1110 mL g^{-1}. Theoretically, the complete reaction of 1 g Al would be expected to produce 1336 mL of H_2 at 25 °C and 1 atm. The 50% yield of hydrogen occurred at 243, 207, 207, 186 and 166 min, respectively. The maximum hydrogen generation rate was 5.3 mL $min^{-1}\cdot g^{-1}$ when $x_{Fe-B} = 0.07$ g. The Co–B had previously shown excellent catalytic activity in $NaBH_4$ hydrolytic that was higher than that of the Ni–B and Fe–B because of its coordinated unsaturated sites [13]. However, it showed low catalytic behavior at 45 °C in the initial corrosion of Al. The induction time was ~60 min and the amount of hydrogen generated was 650 mL g^{-1} for $x_{Co-B} = 0.01$ g. The induction time was shortened to ~22 min and the amount of hydrogen generated was increased to 710 mL g^{-1}

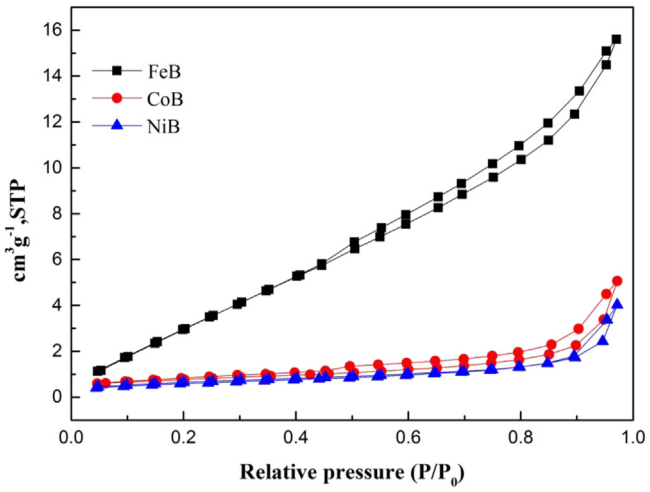

Fig. 4. N_2 adsorption–desorption isotherms of Fe–B, Co–B and Ni–B.

when x_{Co-B} = 0.02 g. The 50% yield of hydrogen occurred at 385 min induced by Co–B (x_{Co-B} = 0.02 g). The amount of hydrogen generated markedly decreased with further increase in the amount of Co–B. The induction time was shortened with increasing Ni–B content, but the amount of hydrogen generated in 400 min monotonically decreased from 895 to 740 mL g^{-1} when the Ni–B content was varied from x_{Ni-B} = 0.02 to x_{Ni-B} = 0.07 g (Fig. 4b). Here, the 50% yield of hydrogen occurred at 236, 269, 268, 313 and 319 min, respectively.

The corrosion of Al mixture in water depended on the electrochemical corrosion [14] or the potential of the metal [15]. In this case, the micro galvanic cells consisted of the M–B (M = Fe, Co, Ni) catalysts and Al, which stimulated the corrosion of Al and generated hydrogen. As aforementioned, the Fe–B network was a mixture of Fe and Fe–B. Not only Fe–B/Al but also Fe/Al or Fe–B/Fe might have formed micro galvanic cells that favor hydrogen generation. On the other hand, Castilho predicted that OH was strongly chemisorbs on the Fe (100) sites, producing a large charge transfer from the surface to *p*-orbitals of the O atoms [15]. This behavior may weaken the OH–H bond. Moreover, the large specific surface area of Fe–B catalyst (169.7 m^2 g^{-1}) provides more numerous active sites for the formation of the micro galvanic cells or for binding between OH^- and Fe. These factors favor the corrosion of Al. The specific surface areas of Co–B (23.6 m^2 g^{-1}) and Ni–B (21.0 m^2 g^{-1}) are smaller than that of Fe–B because of aggregation of Co–B and Ni–B particles, thus explaining their relatively weak catalytic activity compared with that of Fe–B. A uniform dispersion of Co–B or Ni–B was crucial to their catalytic activity [16]. Therefore, Ni–B showed catalytic activity higher than that of Co–B and the sequence of catalytic behavior in the initial Al/H_2O reaction was as follows: Fe–B > Ni–B > Co–B.

The effect of temperature on the Al/H_2O reaction in the presence of 0.02 g of catalyst (Fe–B, Co–B, Ni–B or Al) is shown in Fig. 6. The rate of hydrogen generation by the Al/H_2O reaction induced Fe–B, Ni–B and Co–B particles increased and the induction time shortened. The maximum reaction rate at 35 °C with Fe–B, Co–B and Ni–B were 2.6, 1.5 and 3.4 mL min^{-1} g^{-1}, respectively. These rates increased to 10, 8.5 and 8 mL min^{-1} g^{-1}, respectively, at 65 °C. The apparent activation energy (E_a) of the induced Al/H_2O reaction was calculated through the Arrhenius equation (equation (1)), in which *k* is the maximum chemical reaction rate and *T* is the absolute temperature. A plot of ln *k* against the reciprocal of the absolute temperature (1/*T*) is shown in Fig. 6. Value of the apparent activation energy was calculated from the slope of the straight line. These were found to be 38.2, 39 and 29.6 kJ mol^{-1}for the reaction with Fe–B, Co–B and Ni–B, respectively. These results illustrates that the addition of these catalysts resulted in the decrease in E_a and enhanced the Al/H_2O reaction.

$$\ln k = -\frac{E_a}{RT} + \ln A \quad (1)$$

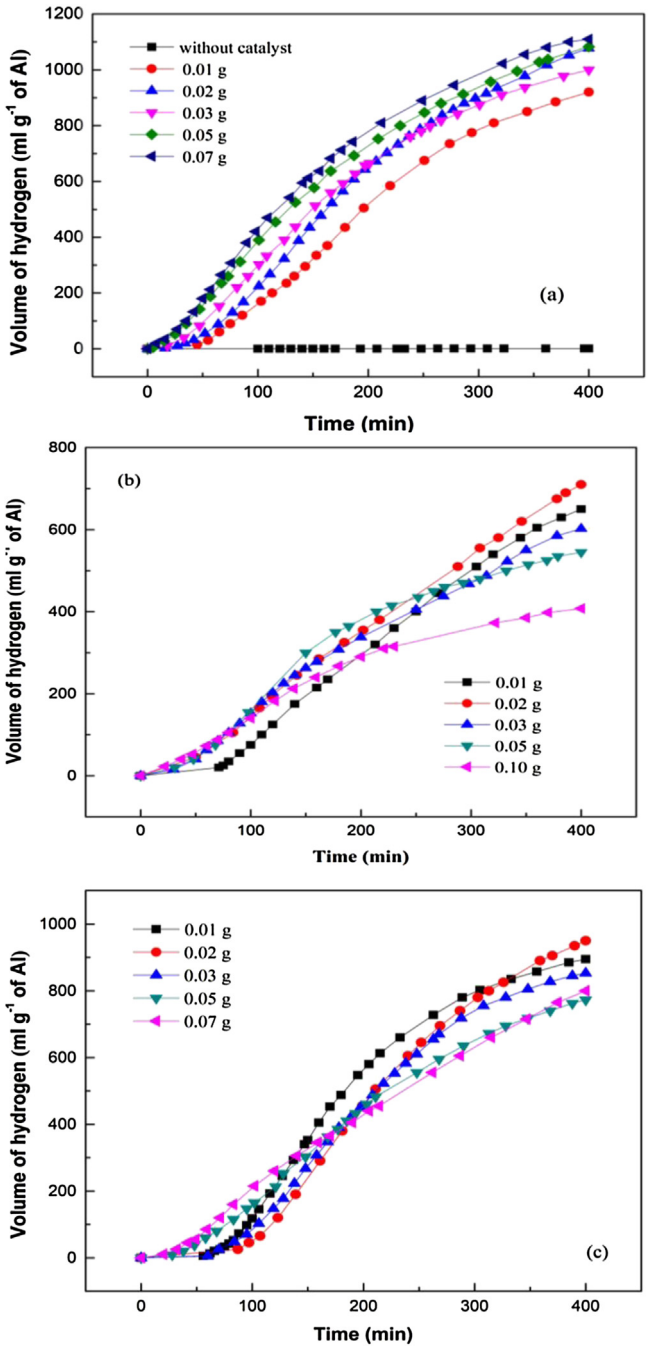

Fig. 5. Hydrogen generation curve at 45 °C by Al/H_2O reaction in the presence of Fe–B (a), Co–B (b) and Ni–B (c).

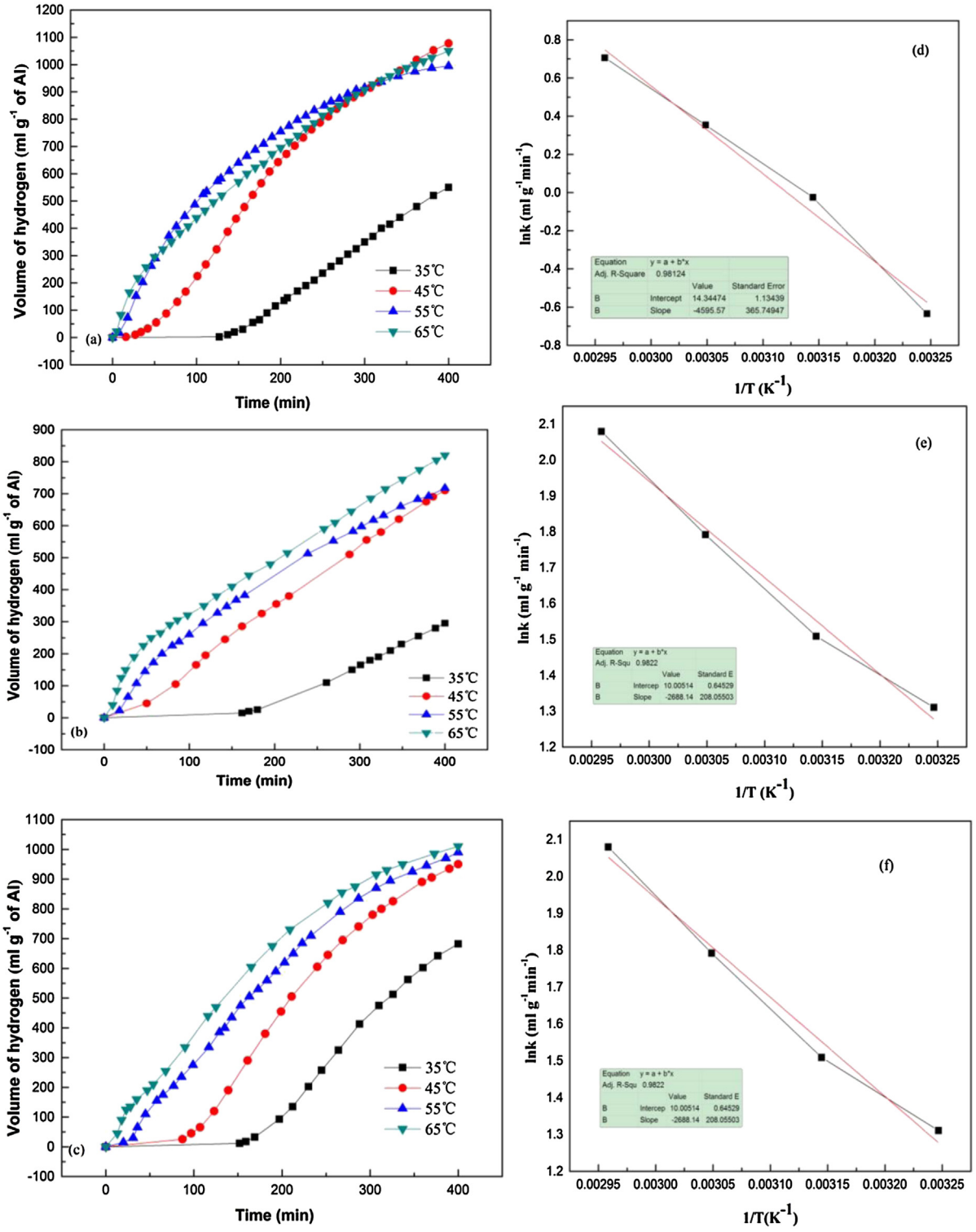

Fig. 6. Effect of the temperature on Al/H_2O reaction in the presence of Fe–B (a,d), Co–B (b,d) and Ni–B (c,f).

3.3. *Effect of consecutive addition batches of Al*

The amount of hydrogen generated by the Al/H_2O reaction induced by Fe–B within 400 min was close to the amounts generated in subsequent additions of Al batches. However, hydrogen evolution started nearly instantaneously (without induction time) after subsequent additions of Al, as shown in Fig. 7. The 50% yield of hydrogen occurred at 104 min upon the first addition of pristine Al, accompanying an increase in average pH from 7.10 to 8.70 (Fig. 7a). Fifty percent of hydrogen in the 2nd, 3rd and 4th batches was 96, 96 and 84 min, respectively. A similar trend was observed with the consecutive 5th, 6th, 7th and 8th batches.

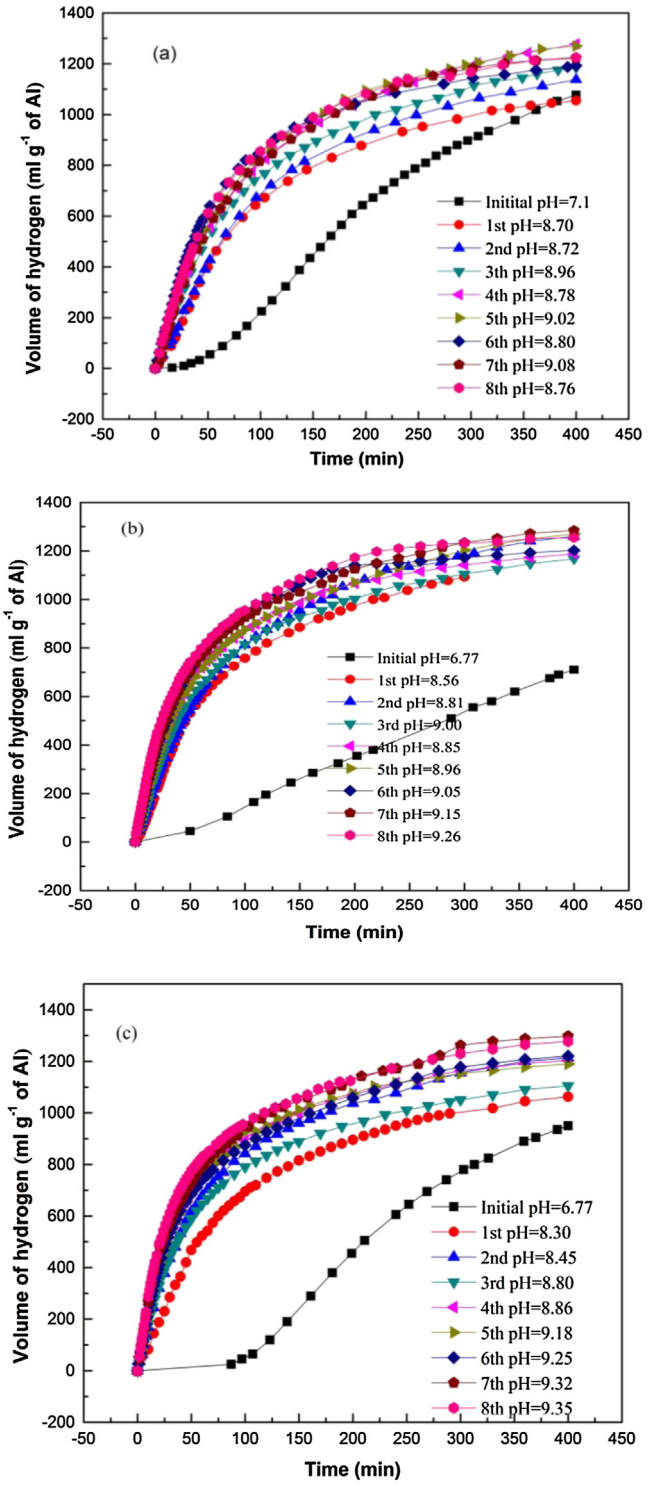

Fig. 7. Hydrogen generation curve in the consecutive batches of pristine Al at 45 °C (a) Fe–B, (b) Co–B (c) Ni–B.

Because the dissociation constant of $Al(OH)_3$ at room temperature is 1.38×10^{-9}, which makes the average pH value of the solution remained between 8 and 10 in the following reaction. Although the initial Al/H_2O reaction with Ni–B or Co–B was not as fast as that with Fe–B, it had higher rates of hydrogen generation with consecutive addition of Al batches. In particular, the 50% yield of hydrogen generation for the 1st, 2nd and 3rd of Co–B is 75, 65 and 65 min, respectively. It was reached in less than 60 min in 4th, 5th, 6th, 7th and 8th batches. This difference might be related to the disruption of the network structure. Nevertheless, rapid generation of hydrogen indicates that the accumulation of $Al(OH)_3$ formed in situ played an important role in Al/H_2O reaction with consecutive addition of Al.

3.4. Reaction mechanism

$$Al + 3OH^- \rightarrow Al(OH)_3 + 3e \quad (2)$$

$$2H_2O + 2e = H_2 + 2OH^- \quad (3)$$

$$Al_2O_3 + 2OH^- + 3H_2O \rightarrow 2Al(OH)_4^- \quad (4)$$

Removal of alumina film at the initial reaction is easy because of the emergence of a micro galvanic cell due to the addition of the M–B (M = Fe, Co, Ni) catalyst. Al acts as an anodes (Equation (2)) and H_2O is the cathode, which undergoes reduction to H_2 (Equation (3)) in the initial Al/H_2O reaction induced by these catalysts. When the oxide film on aluminum is corroded at some points in the initial process, the rapid corrosion of Al occurs [17]. No peaks of $Al(OH)_3$ are present besides the peaks of Al (Fig. 8(A)), when the reaction proceeded within 100 min (225 mL g^{-1} H_2), indicating the poor crystallinity of $Al(OH)_3$. Within this duration a uniform cotton like $Al(OH)_3$ layer covered the aluminum (Fig. 8(B) b), indicating that the oxide film had been destroyed. The cotton like $Al(OH)_3$ layer increased in size and acquired a rod like morphology at the end of the reaction induced by Fe–B(Fig. 8(B) c). In this case, both $Al(OH)_3$ and Al were detected. The rod like $Al(OH)_3$ layer broke down and accumulated in the subsequent Al/H_2O reaction. Only $Al(OH)_3$ was detected after consecutive additions of Al batches. This observation implies that aluminum was rapidly and completely consumed in the saturated solution of $Al(OH)_3$. Al at pH values of about 5–9 has been reported to passivated by a compact film of oxide and hydrated oxide [18]. Wang proposed that the fine and poorly crystalline β-$Al(OH)_3$ with a large surface area may simply release OH^- and H^+ ions that destroy the oxide film and thereby promote the corrosion of Al [19]. However, Deng regarded that the in situ formed finer $Al(OH)_3$ led to a good γ-Al_2O_3 coverage on Al [20]. With the constant release of H_2, the accumulative OH^-concentration in the interface between Al and the oxide film is higher than the detected average value (pH < 10) in this saturated solution. The higher concentration of OH^- triggers the dissolution of Al_2O_3 oxide layer (Equation (4)) and increased corrosion of Al after consecutive additions of Al batches. On the other hand, the thickness of this oxide film is decreased with increasing pH [21]. Moreover, the accumulated $Al(OH)_3$ is not compact, allowing the diffusion of H_2O and OH^- ions at the Al/water interface [22]. This facilitates water to diffuse though the alumina film on Al surface to initiate Al/H_2O reaction.

4. Conclusions

In this work, the Al/H_2O reaction induced by Fe–B, Co–B and Ni–B and the hydrogen generation after the consecutive addition of Al batches have been investigated. The initial Al/H_2O reaction in the presence of Fe–B, Co–B and Ni–B is accelerated by the emergence of a micro galvanic cell due to the formation of an Fe–B network with the larger specific surface area. The apparent activation energy E_a of the Al/H_2O reaction in water under such condition is lower compared with that in other condition. Hydrogen is rapidly produced after consecutive additions of Al batches. Hydrogen

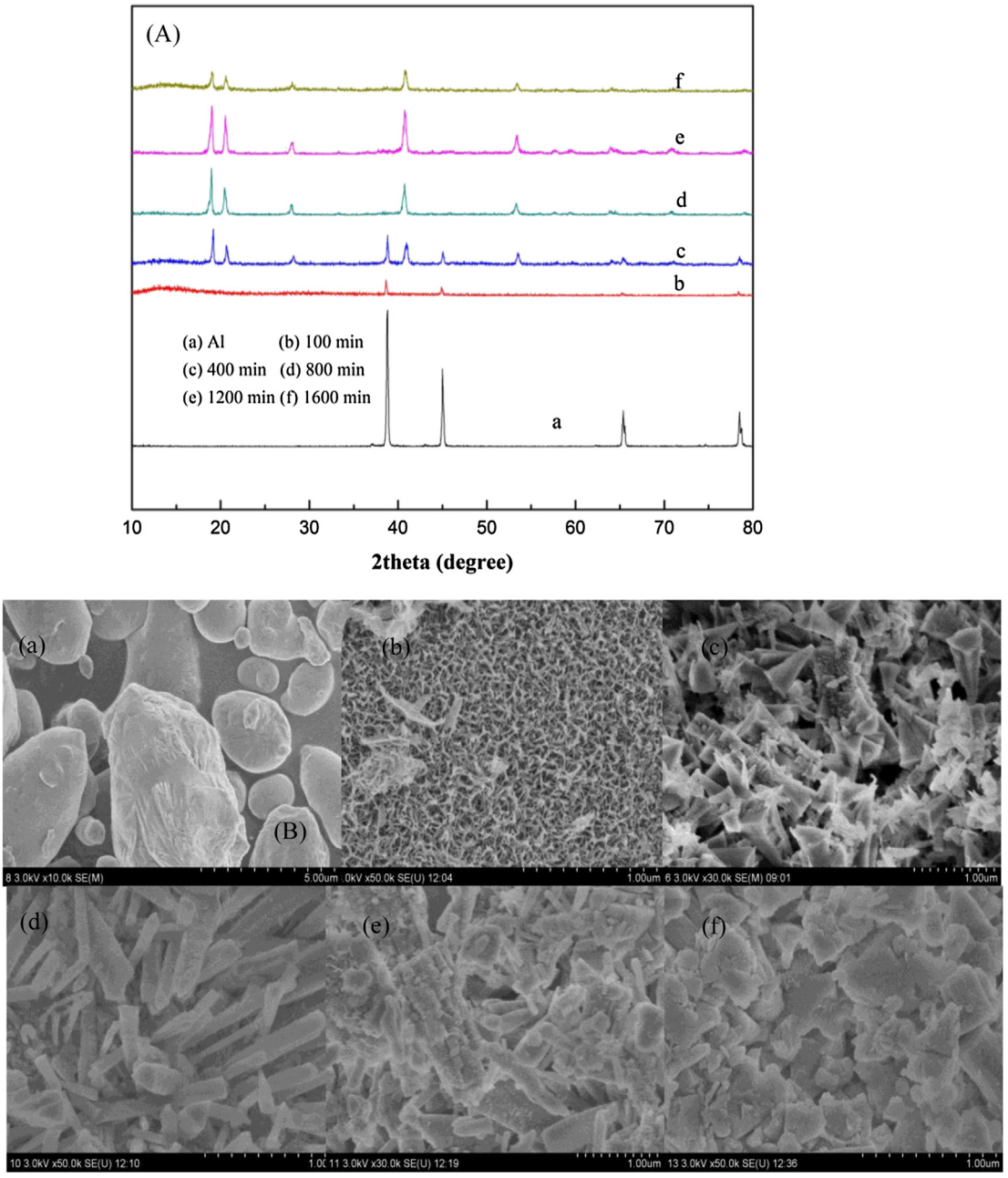

Fig. 8. XRD (A) and SEM (B) of Al and the byproduct.

production leads to a local domains with a high concentrations of $OH^-$and to accumulation of loose $Al(OH)_3$, triggering the rapid corrosion of Al_2O_3 and Al.

References

[1] D. De la Furente, E. Otero-Huerta, M. Morcillo, Corros. Sci. 49 (2007) 3134–3148.
[2] L. Soler, A.M. Candela, J. Macanas, M. Munoz, J. Casado, Int. J. Hydrogen Energy 34 (2009) 8511–8518.
[3] L. Soler, A.M. Candela, J. Macanas, M. Munoz, J. Casado, Int. J. Hydrogen Energy 35 (2010) 1038–1048.
[4] M.Q. Fan, S. Liu, C. Wang, D. Chen, K.Y. Shu, Fuel Cell 12 (2012) 642–648.
[5] X.N. Huang, T. Gao, X.L. Pan, D. Wei, C.J. Lv, L.S. Qin, Y.X. Huang, J. Power Sources 229 (2013) 133–140.
[6] M.Q. Fan, L.X. Sun, F. Xu, Energy 35 (2010) 1333–1337.
[7] Z.G. Wei, W.H. Liu, Z.Y. Deng, J.G. Zhou, Int. J. Hydrogen Energy 37 (2012) 13132–13140.
[8] Z.Y. Deng, J.M.F. Ferreira, Y. Sakka, J. Am. Ceram. Soc. 91 (2008) 3825–3834.
[9] P. Dupiano, D. Stamatis, E.L. Dreizin, Int. J. Hydrogen Energy 36 (2011) 4781–4791.
[10] B.H. Liu, Z.P. Li, J. Power Sources 187 (2009) 527–534.
[11] M. Zhao, T.L. Church, A.T. Harris, Appl. Catal. B 101 (2011) 522–530.
[12] R. Fernanes, N. Patel, A. Miotello, M. Filippi, J. Mol. Catal. A Chem. 298 (2009) 1–6.
[13] N. Patel, R. Fernanes, A. Miotello, J. Catal. 271 (2010) 315–324.
[14] M.Q. Fan, S. Liu, L.X. Sun, F. Xu, S. Wang, J. Zhang, D.S. Mei, F.L. Huang, Q.M. Zhang, Int. J. Hydrogen Energy 37 (2012) 4571–4579.
[15] R.R.Q. Freitas, R. Rivelino, F.D.B. Mota, C.M.C. de Castilho, J. Phys. Chem. C 116 (2012) 20306–20314.
[16] J. Wang, Z.Y. Wang, W. Ke, Mater. Chem. Phys. 139 (2013) 225–232.
[17] F. Zhang, J.S. Pan, C.J. Lin, Corros. Sci. 51 (2009) 2130–2138.
[18] E. Czech, T. Troczynski, Int. J. Hydrogen Energy 35 (2010) 1029–1037.
[19] H.T. Teng, T.Y. Less, Y.K. Chen, H.W. Wang, G.Z. Cao, J. Power Sources 219 (2012) 16–21.
[20] C.S. Fang, W.Z. Gai, Z.Y. Deng, J. Am. Ceram. Soc. 97 (2014) 44–47.
[21] R.D. Armstrong, V.J. Braham, Corros. Sci. 38 (1996) 1463–1478.
[22] Y.J. Liu, Z.Y. Wang, W. Ke, Corros. Sci. 80 (2014) 169–176.